Role of Aquaporin-4 in Airspace-to-Capillary Water Permeability in Intact Mouse Lung Measured by a Novel Gravimetric Method

Yuanlin Song,*‡ Tonghui Ma*‡, Michael A. Matthay,*‡ and A.S. Verkman*‡

From the *Department of Medicine and ‡Department of Physiology, Cardiovascular Research Institute, University of California, San Francisco, San Francisco, California 94143

abstract The mammalian peripheral lung contains at least three aquaporin (AQP) water channels: AQP1 in microvascular endothelia, AQP4 in airway epithelia, and AQP5 in alveolar epithelia. In this study, we determined the role of AQP4 in airspace-to-capillary water transport by comparing water permeability in wild-type mice and transgenic null mice lacking AQP1, AQP4, or AQP1/AQP4 together. An apparatus was constructed to measure lung weight continuously during pulmonary artery perfusion of isolated mouse lungs. Osmotically induced water flux (J_v) between the airspace and capillary compartments was measured from the kinetics of lung weight change in saline-filled lungs in response to changes in perfusate osmolality. J_v in wild-type mice varied linearly with osmotic gradient size (4.4×10^{-5} cm^3 s^{-1} mOsm^{-1}) and was symmetric, independent of perfusate osmolyte size, weakly temperature dependent, and decreased 11-fold by AQP1 deletion. Transcapillary osmotic water permeability was greatly reduced by AQP1 deletion, as measured by the same method except that the airspace saline was replaced by an inert perfluorocarbon. Hydrostatically induced lung edema was characterized by lung weight changes in response to changes in pulmonary arterial inflow or pulmonary venous outflow pressure. At 5 cm H_2O outflow pressure, the filtration coefficient was 4.7 cm^3 s^{-1} mOsm^{-1} and reduced 1.4-fold by AQP1 deletion. To study the role of AQP4 in lung water transport, AQP1/AQP4 double knockout mice were generated by cross-breeding of AQP1 and AQP4 null mice. J_v were (cm^3 s^{-1} mOsm^{-1} $\times 10^{-5}$, SEM, n = 7–12 mice): 3.8 ± 0.4 (wild type), 0.35 ± 0.02 (AQP1 null), 3.7 ± 0.4 (AQP4 null), and 0.25 ± 0.01 (AQP1/AQP4 null). The significant reduction in P_f in AQP1 vs. AQP1/AQP4 null mice was confirmed by an independent pleural surface fluorescence method showing a 1.6 ± 0.2-fold (SEM, five mice) reduced P_f in the AQP1/AQP4 double knockout mice vs. AQP1 null mice. These results establish a simple gravimetric method to quantify osmosis and filtration in intact mouse lung and provide direct evidence for a contribution of the distal airways to airspace-to-capillary water transport.

key words: water permeability • airways • transgenic mouse • membrane transport • aquaporin-1

INTRODUCTION

Water transport across epithelial and endothelial barriers in lung is important for fluid absorption in the perinatal lung and for airspace hydration in the adult lung (Matthay et al., 1996). Lung water transport also occurs in the formation and resolution of interstitial and alveolar edema in clinical conditions such as heart failure and the acute respiratory distress syndrome. As diagramed in Fig. 1 A, the barriers to water movement between airspace and capillary compartments consist of airway and alveolar epithelia, an interstitial compartment, and microvascular endothelia. Transvascular water movement into the interstitium involves passage across the capillary wall, and water movement into the airspaces from the interstitium requires passage across alveolar or airway walls. Although salt is transported rapidly across the distal airway epithelium, it is generally assumed that the vast majority of water is transported across the alveolar epithelium. The total airway surface area in human lung is ~1.4 m^2, representing ~1% of the alveolar surface area of 143 m^2 (Annernarie and Weibel, 1971; Weibel, 1989). The alveolar epithelium contains type I cells, which cover ~95% of the alveolar epithelial surface but whose function is poorly understood, and type II cells, which actively transport salt (Matalon et al., 1991). The airways consist of columnar epithelial cells, and the complex microvascular network consists of endothelial cells forming individual microvessels (Horsfield, 1981; Murry, 1986; Maya, 1991; Simionescu, 1991).

Water permeabilities have been measured across several of the major barriers in lung. Osmotically driven water movement in the in situ sheep lung was determined from the time course of airspace fluid osmolality, measured by direct fluid sampling, in response to instillation of hypertonic saline into the airspaces (Folkesson et al., 1994). Airspace-capillary water transport was very rapid, indicating high water permeability across the microvascular and epithelial barriers. Subsequently, pleural surface fluorescence methods were developed to measure water transport quantitatively in

Address correspondence to Alan S. Verkman, M.D., Ph.D., Cardiovascular Research Institute, 1246 Health Sciences East Tower, Box 0521, University of California, San Francisco, San Francisco, CA 94143-0521. Fax: 415-665-3847; E-mail: verkman@itsa.ucsf.edu

J. Gen. Physiol. © The Rockefeller University Press • 0022-1295/2000/01/17/11 $5.00
Volume 115 January 2000 17–27
Released online 13 December 1999
http://www.jgp.org

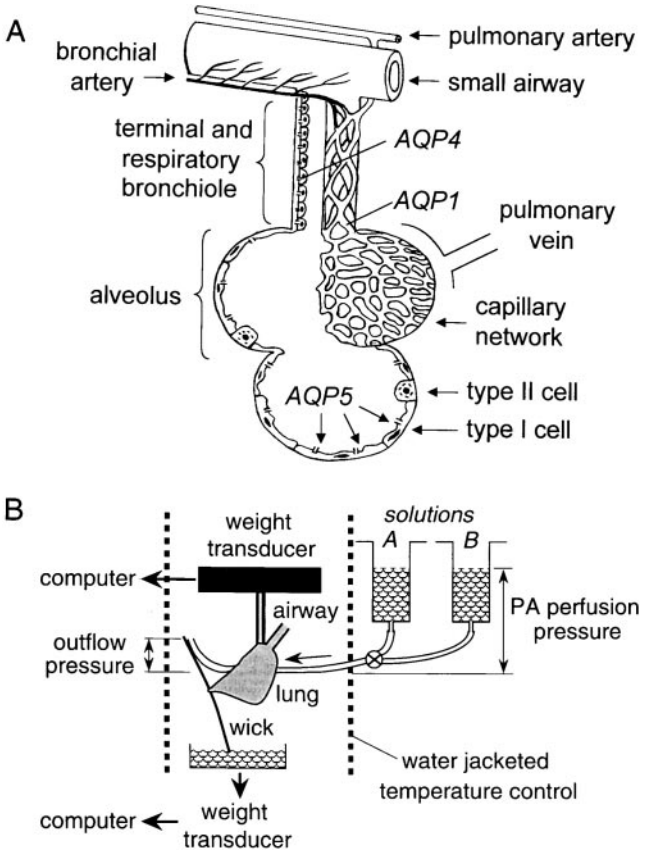

Figure 1. (A) Anatomy of distal lung showing blood supply, airspace epithelia, and locations of aquaporin water channels. Movement of water from the airspace to capillary compartments involves passage across alveolar/airway epithelial, interstitial, and microvascular endothelial barriers. See text for further explanations. (B) Apparatus for continuous measurement of lung weight during perfusion. The airspace compartment is filled with saline or an inert perfluorocarbon via the trachea, and the pulmonary artery perfused with solutions of specified osmolality (solutions A and B) at specified pulmonary artery (PA) perfusion and outflow pressures. Lung weight is measured continuously by a gravimetric transducer and perfusate exit via the transected left atrium or the outflow catheter is measured by second transducer. See text for details.

isolated perfused lungs of small animals, including mice. Osmotically driven water movement between the airspace and capillary compartments was measured by filling the airspaces with a membrane-impermeant fluorescent indicator (Carter et al., 1996). Airspace-to-capillary osmotic water permeability in mouse lung was found to be high (osmotic water permeability coefficient $P_f \sim 0.02$ cm/s), weakly temperature dependent, and mercurial inhibitable. Water permeability in isolated immunopurified type I alveolar epithelial cells was exceptionally high ($P_f \sim 0.07$ cm/s), suggesting a highly water-permeable alveolar epithelial barrier (Dobbs et al., 1998). Water permeability of microvessels in the intact lung was determined by filling the airspaces with an inert perfluorocarbon and perfusing the pulmonary artery with solutions of different osmolalities containing fluorescent indicators (Carter et al., 1998). Osmotic water movement into or out of the microvessels produced prompt changes in pleural surface fluorescence in response to changes in perfusate fluorophore concentration. Microvascular P_f was estimated in mouse lung to be high (0.03 cm/s) using a mathematical model relating the fluorescence change to P_f. In microperfused distal airways from guinea pig, transepithelial airway P_f was determined to be moderately high (0.005 cm/s) and weakly temperature sensitive (Folkesson et al., 1996).

Recent studies in transgenic mice have begun to define the role of aquaporin-type water channels in water transport across the various barriers in the intact lung. Three aquaporins have been localized in lung: aquaporin-1 (AQP1)[1] in microvascular endothelia and some pneumocytes (Nielsen et al., 1993; Folkesson et al., 1994; Effros et al., 1997), AQP4 at the basolateral membrane of airway epithelium (Frigeri et al., 1995), and AQP5 at the apical membrane of type I alveolar epithelial cells (King et al., 1997; Funaki et al., 1998) (Fig. 1 A). AQP1, AQP4, and AQP5 have been deleted in mice by targeted gene disruption (Ma et al., 1997, 1998, 1999). Deletion of AQP1 or AQP5 produced a 10-fold decrease in osmotically driven water transport between the airspace and capillary compartments, and an even greater decrease in transcapillary water permeability (Bai et al., 1999; Ma et al., 2000). AQP1 deletion also caused a moderate decrease in transcapillary water movement in response to hydrostatic pressure differences, but did not affect active near-isosmolar alveolar fluid reabsorption. AQP4 deletion had no significant effect on airspace-to-capillary water permeability or alveolar fluid reabsorption.

The purpose of this study was to determine whether AQP4, and thus the distal airways, contribute measurably to water permeability between the airspace and capillary compartments in intact lung. To be able to detect small effects of AQP4 deletion, measurements were compared in AQP1 null mice, which have low lung water permeability, and double knockout mice in which both AQP1 and AQP4 were deleted. For measurement of water transport, a gravimetric method was developed and validated, which provided a simple and accurate approach to quantify both osmotically and hydrostatically driven water transport across the alveolar–capillary barrier and lung microvessels. The gravimetric method complements and provides distinct technical advantages over pleural surface fluorescence methods (see discussion). Deletion of AQP4 in AQP1 null mice resulted in significantly decreased airspace–capillary water permeability, establishing a role of the airways in lung water transport.

[1]*Abbreviation used in this paper:* AQP, aquaporin.

METHODS

Transgenic Mice

Transgenic knockout mice deficient in AQP1 and AQP4 proteins were generated as described previously (Ma et al., 1997, 1998). Since AQP1 and AQP4 gene loci reside on different chromosomes, AQP1/AQP4 double knockout mice could be generated by serial breeding of AQP1 and AQP4 heterozygous mice to produce double heterozygotes, and then double knockout mice. For comparative measurements in AQP1 null mice with versus without AQP4 deletion, litter-matched mice (8–10 wk of age, 21–32 g body wt) were generated by intercross of AQP1 null mice with AQP4 heterozygous mice in a CD1 genetic background. Genotype analysis of tail DNA was done by polymerase chain reaction at age 5 d. The investigators were blinded to mouse genotype information in comparative transport measurements. A total of 98 wild-type, 35 AQP1 null, 13 AQP4 null, and 12 AQP1/AQP4 double knockout mice were used for the studies reported here. All protocols were approved by the U.C.S.F. Committee on Animal Research.

Isolated Lung Perfusion

Mice were killed using intraperitoneal pentobarbital (150 mg/kg). After a midline incision, the trachea was cannulated in situ with polyethylene PE-90 tubing and the pulmonary artery with PE-20 tubing. The left atrium was usually transected to permit fluid exit, but in some experiments the left atrium was cannulated with PE-20 tubing to set pulmonary venous outflow pressure. After securing the cannulae with 3-0 Nylon suture, the heart, lungs, and trachea were removed en bloc and transferred to a fluorescence microscope or gravimetric apparatus (see below). The pulmonary artery was gravity perfused at specified pressures (generally 20–25 cm H_2O). The time between death and perfusion was generally $<$7 min with $>$80% of perfusions being technically successful. For airspace-capillary water permeability measurements (see below), the airspace was filled with 0.5 ml HEPES-buffered Ringer's (HBR: 137 mM NaCl, 2.68 mM KCl, 1.25 mM $MgSO_4$, 1.82 mM $CaCl_2$, 5.5 mM glucose, 12 mM HEPES, 5% bovine serum albumin, pH 7.4, 300 mosM). For microvascular water permeability measurements, the airspace was filled with 0.5 ml of Fluorinert (3-M), a dense, nonviscous, inert water-immiscible perfluorocarbon.

Pleural Surface Fluorescence Measurements

Osmotically driven water movement between capillary and airspace compartments in surface alveoli was measured by a pleural surface fluorescence method (Carter et al., 1996). In brief, the heart and lungs were positioned on a perfusion chamber for observation by epifluorescence microscopy. FITC-dextran (70 kD, 0.5 mg/ml) was added to the airspace fluid as a fluorescent volume marker. The fluorescence from a 3–5-mm diameter spot on the lung pleural surface was monitored continuously with an inverted epifluorescence microscope using a fluorescein filter set. Signals were detected by a photomultiplier, amplified, digitized, and recorded at a rate of 1 Hz. An airspace-to-perfusate osmotic gradient was generated by switching the perfusate between HBR and HBR containing 0–300 mM sucrose or HBR diluted with water. P_f was computed from the relation: $P_f = [d(F/F_o)/dt]_{t=0}/[(S/V_o)v_w\Delta C]$, where P_f (cm/s) is the osmotic water permeability coefficient, $[d(F/F_o)/dt]_{t=0}$ is the initial slope of the relative fluorescence versus time data, S/V (cm^{-1}) is alveolar surface-to-volume ratio (1,600 cm^{-1}), v_w (18 cm^3/mol) is the partial molar volume of water, and ΔC is the difference in osmolality between perfusate and airspace fluids.

Gravimetric Apparatus

Fig. 1 B shows a schematic of the gravimetric apparatus for continuous measurement of lung weight. The heart/lung block was suspended from a weight transducer (TSD125C; Biopac Inc.) with sensitivity $<$1 mg. The perfusion inflow tubing was positioned so as not to interfere with weight measurements. The perfusate fluid leaving the transected left atrium or left atrial cannula was drawn away from the heart/lung bloc by a wick to avoid artifactual weight changes arising from droplet formation. The wick consisted of a (2 $\times$ 20 mm) strip of waxed weighing paper adherent to the dorsum of the lung. The lower pole of the wick was immersed in fluid in a reservoir that rested on a second weight transducer. Perfusate flow was monitored in every measurement from the increasing reservoir weight. The gravimetric transducers were interfaced to a recorder (MP100A-CE; Biopac Inc.) and PC computer. Data were acquired at a rate of 500 Hz and averaged over 1-s intervals. For temperature control, the heart/lung block was positioned in a custom-designed cylindrical glass chamber (10 cm length, 2.5 cm inner diameter) in a moisturized air atmosphere connected to a circulating water bath. The chamber contained a slot for positioning the perfusion tubing. The gravity-fed perfusion system consisted of reservoirs and valves to permit rapid changes in perfusate fluid composition without transient changes in pressure, or rapid changes in perfusion inflow or outflow pressure. The perfusion tubing proximal to the pulmonary artery insertion point was enclosed in a temperature-jacketed compartment.

Gravimetric Water Permeability Measurements

Osmotically driven water transport between the airspace and capillary compartments was determined from the time course of lung weight in response to changes in pulmonary artery perfusate osmolality. The airspaces were filled with HBR as described above. The hyperosmolar solutions (310–600 mOsm) consisted of HBR containing specified amounts of sucrose, glycine, urea, or NaCl; the hypoosmolar solutions (290–150 mOsm) consisted of HBR diluted with distilled water. The initial change in lung weight following a maneuver, J_w (mg/s), was determined from the derivative (evaluated at zero time) of a quadratic polynomial fitted to the first 1–2 min of weight data. Osmotically driven water transport between the capillary and interstitial compartments was measured as described above except that the airspaces were filled with Fluorinert. Hydrostatically driven water transport (filtration) was measured from the time course of lung weight in response to changes in the inflow pressure of the HBR perfusate (to simulate pulmonary arterial hypertension) or in the venous outflow pressure (to simulate left-sided congestive heart failure).

RESULTS

Gravimetric Measurement of Lung Water Permeability

The gravimetric and pleural surface fluorescence methods were compared for determination of airspace-capillary osmotic water permeability, a measurement that can be made by both methods (Fig. 2, A and B). The pleural surface fluorescence method provides information about the concentration of a fluorophore (proportional to osmolality) in fluid-filled airspaces only very near ($<$200 μm) the lung surface (Carter et al., 1996). Changes in fluorophore concentration are produced by water movement into or out of the airspace compartment across the alveolar or airway epithelial barriers.

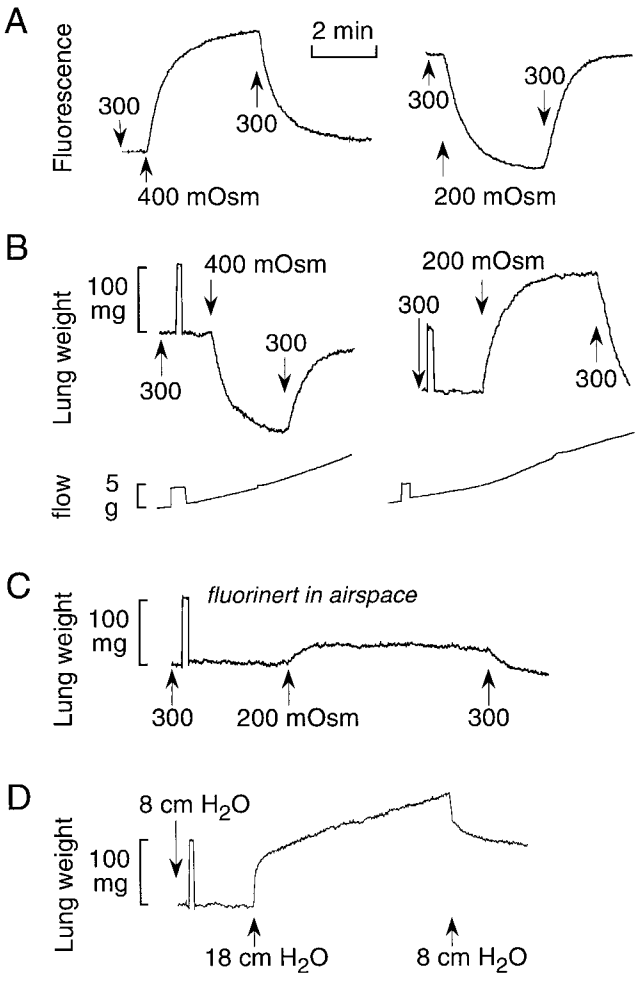

Figure 2. Gravimetric measurement of lung water permeability. (A) Pleural surface fluorescence recordings. The airspace was filled with HBS containing FITC-dextran and the pulmonary artery perfused with solutions of indicated osmolalities (see methods for details). (B) Lung weight was recorded continuously in response to indicated changes in perfusate osmolality. The airspace was filled with HBS. Perfusion pressure was 20 cm H_2O. (Bottom) Perfusate flow shown as the increasing weight of a collection reservoir. (C) Same experiment as in B, except that the airspace was filled with an inert perfluorocarbon. (D) Pulmonary artery was perfused with HBS. Venous outflow pressure was set at 5 cm H_2O and pulmonary artery perfusate pressure was increased from 8 to 18 cm H_2O.

Fig. 2 A shows the reversible increase in pleural surface fluorescence in response to increasing perfusate osmolality from 300 to 400 mOsm (Fig. 2, A and B, left) and the decrease in fluorescence after decreasing osmolality from 300 to 200 mOsm (right).

The gravimetric method measures total lung weight and thus the sum of fluids contained in the airspace, interstitial, and capillary compartments. Averaged information is obtained for the whole lung rather than surface alveoli/vessels, and no exogenous fluorescent probe is used. When the airspace compartment is filled with an isosmolar saline solution, changes in perfusate osmolality result in water movement across endothelial and epithelial barriers, producing changes in interstitial and airspace water content observed as changes in lung weight. Fig. 2 B shows representative gravimetric data for the same changes in perfusate osmolality studied by the fluorescence method. Increasing perfusate osmolality to 400 mOsm (left) produced a decrease in lung weight as water is extracted from the extravascular spaces of the lung; decreasing perfusate osmolality to 200 mOsm (right) had the opposite effect. A 100-mg weight calibration was done in every experiment, as well as real-time measurement of perfusate flow. Detailed characterization of the gravimetric method for measurement of airspace-capillary osmotic water transport is provided below in Figs. 3 and 4.

We showed previously that when the airspace compartment is filled with an inert perfluorocarbon (to minimize fluid movement into the airspaces) and perfusate osmolality is changed, information is obtained regarding osmotically driven water transport across the microvascular barrier (Carter et al., 1998). The fluorescent marker was added to the pulmonary artery perfusate in the capillary compartment. Water movement between the interstitial and capillary compartments across the microvascular endothelial barrier was determined from the rapid change in concentration of the fluorescent marker in response to a change in pulmonary artery perfusate osmolality. Again, the measurement provides information selectively on the osmotic water permeability of surface vessels and, as discussed by Carter et al. (1998), the method provides only semiquantitative or comparative information because of assumptions needed to deduce absolute permeability coefficients from the fluorescence data. Fig. 2 C shows that in the presence of airspace perfluorocarbon, a decrease in perfusate osmolality from 300 to 200 mOsm produces a small, reversible increase in lung weight as fluid accumulates in the interstitial compartment. Because of the physical restrictions of the interstitium, the lung weight change is substantially lower than that in Fig. 2 B, where the airspaces are fluid filled.

The gravimetric method permits measurements of lung fluid transport in response to hydrostatic pressure gradients, measurements that cannot be carried out by a fluorescence approach. Fig. 2 D shows the increase in lung weight in response to a change in pulmonary artery pressure from 8 to 18 cm H_2O at a constant pulmonary venous outflow pressure of 5 cm H_2O. The perfusate consisted of an isosmolar saline solution throughout. Initially, there was a prompt increase in weight resulting from vascular engorgement, which was generally complete in $<$10 s. The vascular phase was followed by a linear increase in weight as extravascular lung fluid accumulates. Reduction of perfusion pressure to 8 cm H_2O produced a rapid weight decrease, due to de-

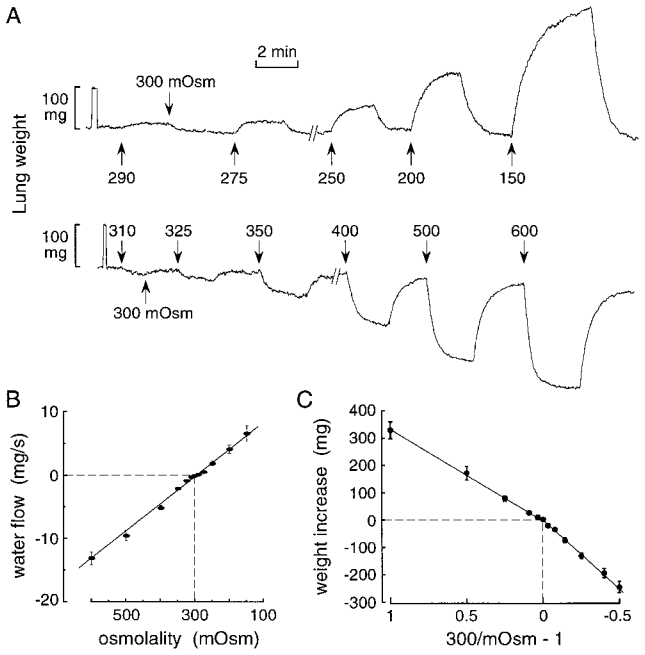

Figure 3. Osmotic gradient dependence of airspace-capillary water transport in perfused lungs of wild-type mice. (A) Representative original weight recordings obtained with indicated perfusate osmolalities. The airspace compartment was filled with isosmolar HBS (0.5 ml) and the pulmonary artery perfused at constant pressure (20 cm H_2O, flow 2.5–3 ml/min) at room temperature. (B) Initial water flow (mean ± SEM, n = 3–6 lungs) as a function of perfusate osmolality. Positive water flow corresponds to movement out of the airspace. (C) Net lung weight increase as a function of 300/mOsm^{-1}, where mOsm is perfusate osmolality. See text for details.

creased vascular engorgement, followed by a slower and not fully reversible decrease in lung weight. Additional characterization of the gravimetric method to measure lung filtration is given in Fig. 5.

Characterization of Lung Water Transport in Wild-Type and AQP1 Knockout Mice

The dependence of osmotically driven water transport on osmotic gradient size and direction was measured from lung weight changes in response to a series of osmotic gradients. The airspace compartment was filled with isosmolar saline and the perfusate fluid was switched between isosmolar and hyperosmolar or hypoosmolar solutions. Fig. 3 A shows that the rates and magnitudes of the weight changes were dependent on osmotic gradient size. Changes in lung weight of <10 mg could be measured in response to osmotic gradients as small as 10 mOsm. Averaged initial rates of lung weight change are given in Fig. 3 B. There was a linear relationship between water flux and osmotic gradient size, with slope 4.4×10^{-5} cm^3 s^{-1} mOsm^{-1} at 23°C, indicating that lung water transport is symmetrical and nonrectifying. Fig. 3 C shows the dependence of lung weight change on osmotic gradient size. The abscissa is expressed as the dimensionless ratio (300 mOsm/perfusate osmolality − 1), derived from the relationship (300 mOsm)w_o = (perfusate osmolality) (w_o + Δw), where w_o is the initial weight of fluid instilled into the airspaces and Δw is the weight gain. As predicted for a simple osmometer, the lung weight change (Δw) varied with 300/mOsm − 1 in a nearly linear manner. A small difference in slope is noted for weight increases versus decreases, which might be related to interstitial and intracellular water accumulation/volume regulation and/or heterogeneity in regional perfusion.

Osmotically driven water permeability was further characterized in terms of effects of osmotic solute size, temperature, and perfusion pressure. Fig. 4 A (left) shows similar lung weight kinetics in response to matched osmotic gradients of NaCl, sucrose, glycine, and urea. Averaged water fluxes (Fig. 4 A, right) indicate that osmotically driven water transport is independent of osmolyte size, indicating unity reflection coefficients for the solutes studied here. The monophasic time course of lung weight change further indicated that the permeability of each solute across the airspace-capillary barrier is very low. Fig. 4 B (left) shows original data from temperature-dependence measurements done on wild-type and AQP1 null mice. Lung water permeability was remarkably decreased (10-fold at 23°C) by AQP1 deletion. Water permeability in wild-type mice was minimally affected by temperature changes in the range 12–37°C. The averaged water fluxes are summarized in an Arrhenius plot (Fig. 4 B), giving apparent activation energies (E_a) of 2.4 (wild-type mice) and 7.6 (AQP1 null mice) kcal/mol. The higher E_a in AQP1 null mice is consistent with water movement via a rate-limiting lipid- rather than channel-mediated pathway. Fig. 4 C shows the effect of pulmonary artery perfusion pressure on changes in lung weight in response to osmotic gradients. A series of such measurements indicated that a pulmonary artery pressure of 18 cm H_2O, corresponding to an average flow of 2.5 ml/min, was able to induce maximal (vascular flow-independent) water transport. Fig. 4 D shows the effect of increasing left atrial pressure at a constant 20 cm H_2O inflow–outflow pressure difference. Although increased pressure resulted in lung water accumulation (see below), osmotic water permeability remained unchanged.

Fig. 4 E shows the effect of AQP1 deletion on lung microvascular water permeability in which perfusate osmolality was changed in the presence of fluorinert-filled airspaces. AQP1 deletion produced slowed lung fluid accumulation in response to the osmotic gradient, consistent with a marked reduction in microvascular endothelial water permeability. The increase in lung weight was too small to quantify the residual water permeability after AQP1 deletion.

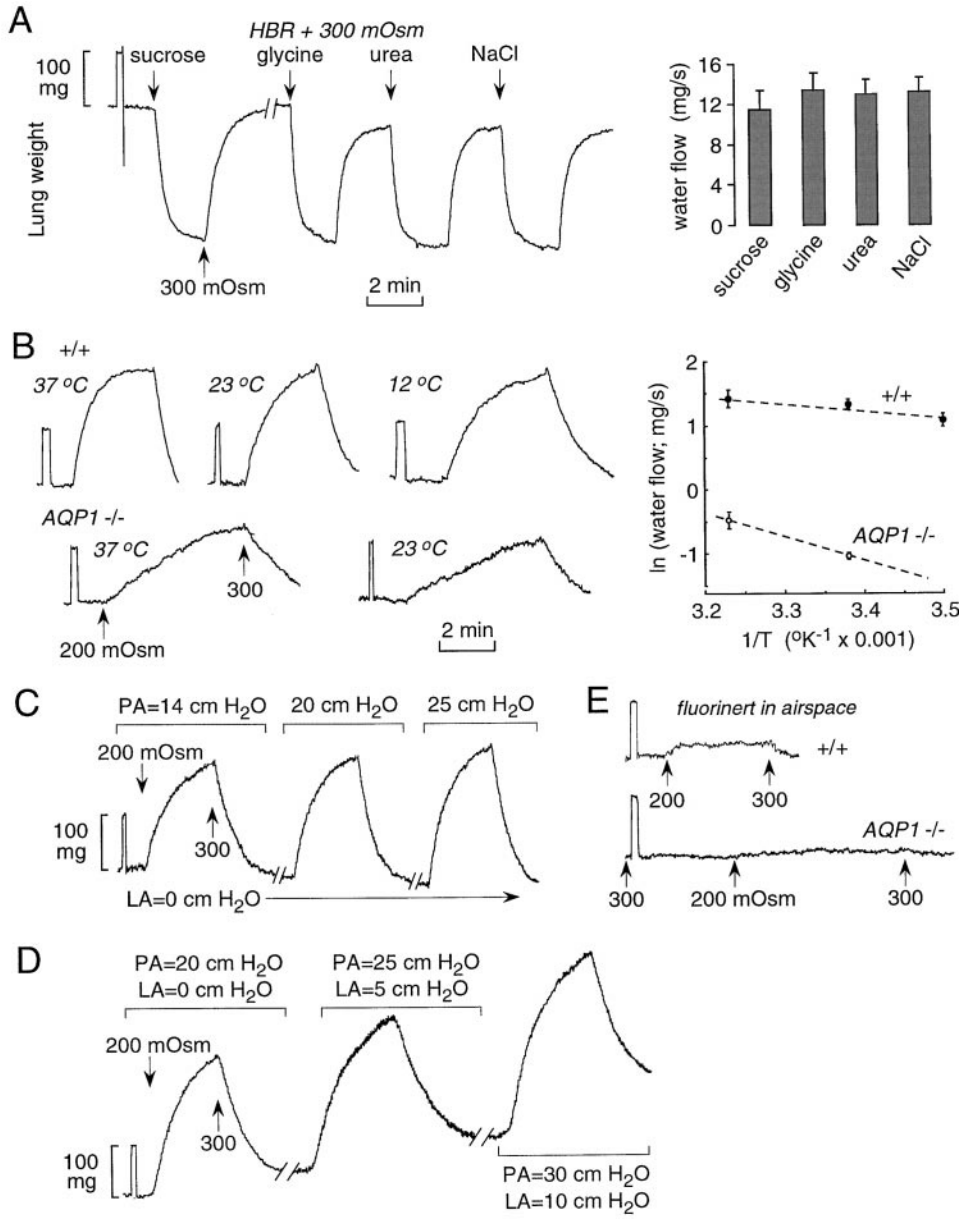

Figure 4. Characterization of airspace-capillary osmotic water transport. (A) Dependence of osmotically driven water transport on osmolyte size. The airspace compartment was filled with isosmolar HBS and the perfusate solutions switched between HBS and hyperosmolar HBS containing 300 mOsm NaCl, urea, glycine, or sucrose as indicated. Original gravimetric recordings are shown at the left and averaged water flow data at the right. (B) Temperature-dependence measurements were done as in A, using NaCl as osmolyte, in wild-type and AQP1 null mice. Original gravimetric recordings are shown at the left and an Arrhenius plot at the right. (C and D) Effect of pulmonary artery (PA) perfusion pressure and left atrial (LA) outflow pressure. Perfusate osmolalities were changed from 300 to 200 mOsm at indicated perfusion pressures. (E) Effect of AQP1 deletion on microvascular water permeability. The airspace was filled with an inert perfluorocarbon and the pulmonary artery perfused with solutions of indicated osmolalities. See text for explanations.

Fig. 5 shows the effect of AQP1 deletion on lung fluid accumulation in response to hydrostatic driving forces. Previously, we reported qualitative differences in lung fluid accumulation with AQP1 deletion when venous outflow pressure was kept at zero (transected left atrium) (Bai et al., 1999). Similar measurements in Fig. 5 A show a vascular engorgement phase followed by a slower saturable increase in lung weight. The slower increase in lung weight was attenuated in the AQP1 null mice. Two concerns with these studies include the difficulty in unambiguously identifying vascular versus lung edema phases, and the difficulty in performing quantitative analysis because of saturable lung water accumulation. Similar concerns were raised in filtration measurements of fluid accumulation in perfused dog lungs in response to increases in pulmonary venous pressure (Parker et al., 1993). We have now been able to cannulate the left atrium in mice to set pulmonary venous outflow pressure. Fig. 5 B shows the effect of increasing left atrial outflow pressure at constant pulmonary artery inflow pressure. There was a saturable increase in lung weight representing a combination of vascular engorgement and extravascular fluid accumulation.

Fig. 5 C shows that at a constant outflow pressure of 5 cm H_2O, an increase in perfusion pressure from 8 to 18 cm H_2O produced a prompt increase in lung weight (vascular engorgement) that is easily distinguished from a nearly linear slower increase in lung weight. The continued accumulation of lung water is probably related to the effective contribution of post-capillary fil-

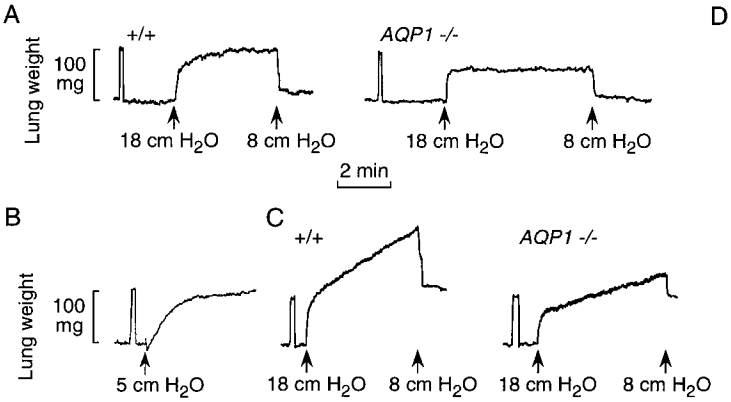

Figure 5. Characterization of hydrostatic lung edema. The pulmonary artery was perfused with isosmolar HBS. (A) Time course of lung weight in response to changes in perfusate pressure at zero venous outflow pressure. Initial perfusate pressure was 8 cm H_2O. (B) Perfusate pressure was set at 8 cm H_2O and venous outflow pressure was increased from 0 to 5 cm H_2O. (C) Same as in A, except that venous outflow pressure was kept at 5 cm H_2O. (D) Summary of the rate of weight accumulation (slope of linear weight increase) from individual mice studied as in C. $*P < 0.05$ (unpaired t test).

tration when left atrial pressure is elevated, which more closely recapitulates the in vivo situation. Averaged rate of lung water accumulation was 0.63 ± 0.05 mg/s, giving a filtration coefficient of 4.7 ml min^{-1} cm H_2O^{-1}/100 g wet lung wt. AQP1 deletion produced a slower rate of lung water accumulation (Fig. 5 C, right).

The linear increase in lung water accumulation permitted quantitative comparisons of hydrostatically driven edema formation in wild-type versus AQP1 null mice (Fig. 5 D). There was a small but significant decrease in lung water accumulation in the null mice, despite the dramatic reduction in osmotically driven water transport seen in Fig. 4 B.

Role of AQP4 in Lung Water Permeability

To determine the role of AQP4 in airspace-capillary water transport, osmotic water transport was compared in perfused lungs of wild-type, AQP1 knockout, AQP4 knockout, and AQP1/AQP4 double knockout mice. The AQP1 knockout and AQP1/AQP4 double knockout mice were carefully matched in body weight and the investigator was blinded to mouse genotype until completion of the analysis. Lungs from wild-type, AQP1 knockout, and AQP1/AQP4 double knockout mice were indistinguishable grossly and by light microscopic examination. Survival of the single and double knockout mice was excellent and similar to that of wild-type mice; however, the AQP1 knockout mice generally grew 10–13% slower than wild-type mice and the AQP1/AQP4 double knockout mice grew 15–20% slower than wild-type mice.

Fig. 6 A shows representative original weight recordings for mice of each genotype. Whereas AQP4 deletion had no obvious effect on water transport (compared with wild-type mice), there was a consistent difference in water transport in lungs of AQP1 knockout versus AQP1/AQP4 double knockout mice. A full set of measurements was done on a separate set of mice using the pleural surface fluorescence method with representative recordings shown in Fig. 6 B. There was a consistently lower rate of water transport in lungs from the double knockout mice compared with the AQP1 knockout mice, in agreement with the gravimetric data.

Averaged osmotically driven volume fluxes for individual mice determined from gravimetric and pleural surface fluorescence measurements are summarized in Fig. 7, A and B, respectively. There was no significant ef-

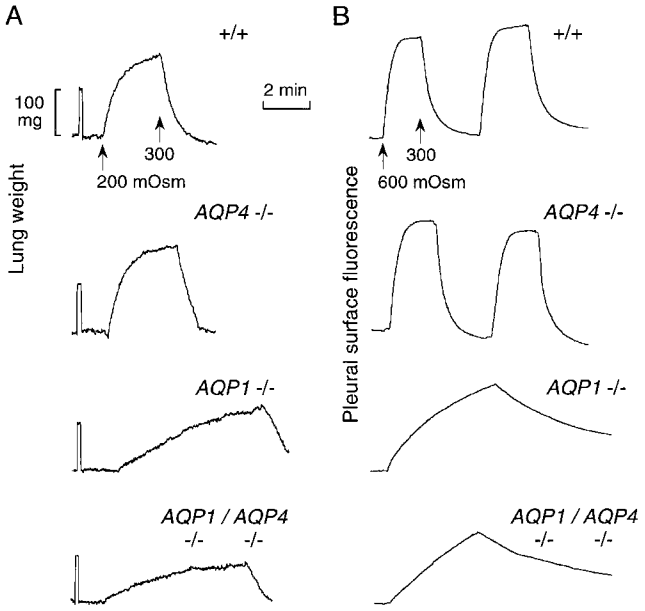

Figure 6. Effects of AQP1 and AQP4 deletion on airspace-capillary water transport. (A) Representative weight recordings for measurements done as in Fig. 2 B for perfusate osmolalities of 300 and 200 mOsm. (B) Representative pleural surface fluorescence recordings for measurements done as in Fig. 2 A for perfusate osmolalities of 300 and 600 mOsm.

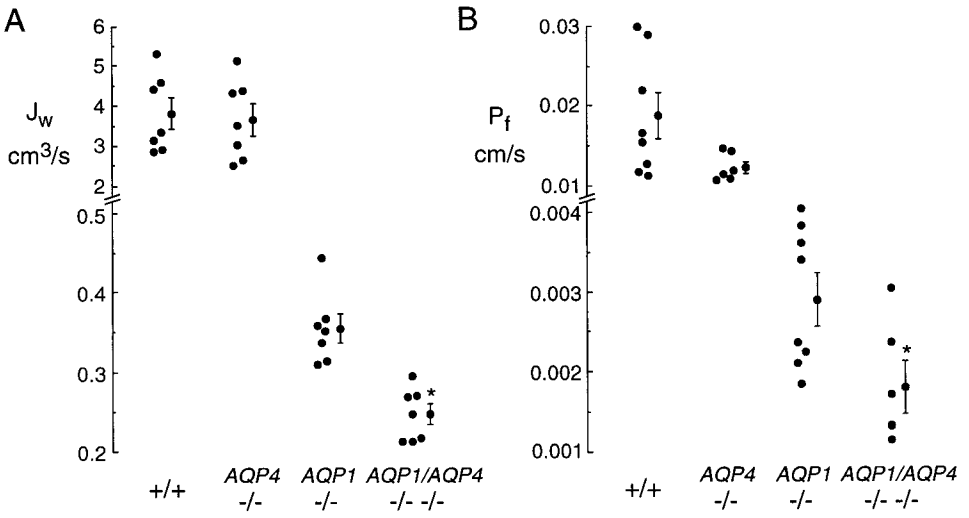

Figure 7. Role of AQP4 in airspace-capillary water permeability. Summary of gravimetric (A) and pleural surface fluorescence (B) measurements. Each point represents averaged measurements made on an individual mouse. Averaged data (mean ± SEM) shown.

fect of AQP4 deletion in wild-type mice, whereas AQP4 deletion in AQP1 null mice (comparing AQP1 knockout and AQP1/AQP4 double knockout mice) produced a 1.44-fold decrease in water permeability ($P < 0.001$, gravimetric study; $P < 0.05$, fluorescence study). Compared with wild-type mice, AQP1 deletion produced a 10-fold decrease in water permeability, and AQP1/AQP4 deletion produced a 15.3-fold decrease.

DISCUSSION

As reviewed in the INTRODUCTION, recent studies have defined the water transporting properties of the permeability barriers in lung. Water permeabilities of the alveolar epithelial and microvascular endothelial barriers are very high as measured in sheep, rat, and mouse lung, whereas the water permeability of isolated distal airways (measured in guinea pig lung) is substantially lower. Technical limitations in the microperfusion methods have precluded the measurement of airway water permeability in mammals other than guinea pig. The role of aquaporin water channels is of considerable interest for lung fluid balance in the perinatal and adult lung, both under normal and pathological conditions. Because there are at present no aquaporin inhibitors for in vivo use, the generation of knockout mice lacking specific aquaporins was undertaken to investigate the role of aquaporins in organ physiology. Transgenic mice lacking AQP1 are unable to concentrate their urine (Ma et al., 1998) because of defective functioning of the proximal tubule (Schnermann et al., 1998) thin descending limb of Henle (Chou et al., 1999), and vasa recta (Pallone et al., 2000), whereas mice lacking AQP4 have a mild defect in urinary concentrating ability (Ma et al., 1997) despite a fourfold decreased water permeability in the inner medullary kidney collecting duct (Chou et al., 1998). An initial study in lung showed that AQP1 deletion produced an ~10-fold decrease in osmotically driven water transport between the airspace and capillary compartments, whereas AQP4 deletion had no significant effect (Bai et al., 1999). The current study focuses on the role of AQP4 in lung water transport, mandating the development of a sensitive gravimetric method to quantify lung water permeability in mice.

The contribution of airway AQP4 to airspace-capillary water permeability was investigated by comparing water transport in mice lacking AQP1 alone versus AQP1 and AQP4 together. It was reasoned that the relatively low lung water permeability in AQP1 null mice might permit the detection of a small incremental effect of AQP4 deletion. AQP1/AQP4 double knockout mice were generated by breeding of mice containing the individual gene deletions. Airspace-capillary water permeability, measured by the established pleural surface fluorescence method as well as a new gravimetric method, was significantly reduced by 1.4–1.6-fold in AQP1/AQP4 double knockout mice versus AQP1 knockout mice. No significant effect of AQP4 deletion in wild-type mice was found, probably because of the substantially greater basal water permeabilities. The 1.4–1.6-fold effect of AQP4 deletion on water permeability in the AQP1 null mice suggests an overall contribution of AQP4 to lung water permeability of ~4% (taking into account the 10-fold effect of AQP1 deletion alone). Although this represents a relatively small contribution, it is remarkably greater than that predicted based on estimates that the airways comprise only 1.4% of the total airspace epithelial surface area (Horsfield, 1981; Weibel, 1989) and that transepithelial water permeability in airways is 5–10-fold lower than across alveoli (Folkesson et al., 1996). These data suggest that the airways may have a greater role in net lung

fluid transport than previously anticipated, especially given their relatively active role in salt transport.

AQP4 expression is strongly upregulated in the neonatal period, a time where rapid absorption of distal airspace fluid occurs and when relatively little AQP1 and AQP5 are expressed (King et al., 1996; Umenishi et al., 1996; Yasui et al., 1997). The corresponding increase in airspace-capillary water permeability measured in rabbit lung within the first day after birth (Carter et al., 1997) might thus involve increased AQP4 expression. However, technical limitations in applying the gravimetric and fluorescence methods in neonatal mouse lung preclude experimental verification of this hypothesis at present.

Because of the complex airspace and microvascular geometry, it is difficult to quantify effective airway versus alveolar surface areas, as well as fluid flow patterns during osmosis. As depicted in Fig. 1 A, the pulmonary artery runs with the airways and divides as the airways divide. A capillary bed consisting of AQP1-containing endothelial cells is formed in the alveolar acinar region beyond the terminal bronchiolus. The bronchial artery forms a capillary plexus that supplies the muscle and submucosa of the airways. This plexus communicates with branches of the pulmonary artery and empties into the pulmonary veins. In addition, there is further complexity in terms of heterogeneity in microvasculature and alveolar geometry in different regions of the lung. Thus, the description of lung fluid movement in terms of passage across well-demarcated geometric barriers is probably an oversimplification, underscoring the need for functional studies to quantify barrier properties.

Gravimetry is a classical method to study organ bed capillary filtration that originated more than 50 years ago (Pappenheimer and Soto-Rivera, 1948) and first used in lung in 1962 (Agostoni and Piiper, 1962). Gravimetry has been used to measure hydrostatic capillary filtration in dog lung (Gaar et al., 1967; Ehrhard et al., 1984; Harris et al., 1992; Parker et al., 1993). For measurements of lung filtration in large animals, the pulmonary artery is generally perfused using a constant flow infusion pump, and lung weight is measured in response to increased venous outflow pressure. As found here in mice, the kinetics of weight increase consist of a relatively rapid phase, corresponding to vascular engorgement, followed by a slower phase corresponding to lung fluid accumulation. Because of ambiguity in identifying the vascular versus edema accumulation phases, various deconvolution and other approaches were developed to analyze the data in dog lung. For the mouse studies done at a constant 5 cm H_2O venous outflow pressure, the two phases appear to be well demarcated. The "filtration coefficient" in dog lung has been reported to be in the range 0.02–1.5 ml min^{-1} cm H_2O^{-1}/100 g wet lung wt depending on detailed conditions and measurement methods (Gaar et al., 1967; Drake et al., 1980; Parker et al., 1993). In the measurements done here in mice, a 10-cm H_2O pressure gradient produced a filtration rate of 0.0038 ml/min, which in the units reported for dog lung is 4.7 ml min^{-1} cm H_2O^{-1}/100 g wet lung wt. Thus the filtration rate, as well as other details of the kinetics of lung weight change, are quite different in mouse versus dog. These findings underscore the need to establish water permeability and fluid filtration properties in mouse lung, which has become an important model since the availability of transgenic mice.

An interesting observation in the hydrostatic edema studies was that interstitial fluid accumulation was strongly dependent on venous outflow pressure. At a venous outflow pressure of zero (transected left atrium), there was mild fluid accumulation that saturated over a few minutes, whereas sustained fluid accumulation occurred when left atrial outflow pressure was maintained at 5 cm H_2O. At zero venous outflow pressure, there was limited edema even when pulmonary artery pressure was increased to 45 cm H_2O (not shown). These results suggest that the venous component of the microvasculature plays an important role in lung fluid accumulation in response to hydrostatic pressure differences. In addition, the increased venous outflow pressure may promote the maintenance of microvascular bed patency throughout the lung. AQP1 deletion was associated with a small, but significant 1.4-fold decrease in lung fluid accumulation in response to a hydrostatic stress, despite a 10-fold reduction in osmotically driven airspace-capillary water permeability. Therefore, AQP1-independent pathways, probably involving paracellular water transport, play a major role in hydrostatically driven transcapillary water movement.

The gravimetric method provides a simple and quantitative approach to characterize the water permeability properties of microvascular and epithelial barriers. The modifications to the classical gravimetric method introduced here for studies in small animals permit measurements of both osmotic and hydrostatically driven lung water transport across airspace-capillary barriers. The administration of perfluorocarbon into the airspaces permits measurements of transcapillary water movement without the confounding effects of transepithelial fluid movement. The instrumentation for gravimetric measurements in small animals is simple, consisting of 2-mg–resolution gravimetric transducers and various reservoirs, values, and heating devices to control and measure perfusate pressure, flow, and composition. Because of the small weight of the mouse lung, care is needed to minimize changes in lung weight arising from solution exiting the lung and evaporative water losses. In contrast to pleural surface fluorescence

measurements, gravimetry permits direct assessment of the fluid content of the interstitial compartment, and provides information about all airspaces rather than only those at the pleural surface. The determination of microvascular water permeability does not require complex experimental and analysis methods. The characterization of hydrostatically driven water transport has not been done previously in mice and cannot be done by fluorescence approaches. The simplicity of the gravimetric apparatus and the straightforward interpretation of experimental data should make it attractive to laboratories studying lung fluid transport in transgenic mice and other small animals.

The application of gravimetry to quantify lung water transport is particularly useful for comparative studies, such as in lungs of wild-type versus transgenic mice, and effects of inhibitors and temperature. As mentioned above, the determination of absolute permeability coefficients (in contrast to apparent permeabilities and filtration coefficients) is challenging because of the complex lung anatomy and potential heterogeneity in perfusion efficiency. There are a number of other concerns for quantitative applications of gravimetry. Unstirred layer effects is a consideration for permeability measurements in organ perfusion models (Verkman, 2000). However, the excellent vascularization and small alveolar size minimizes unstirred layer effects in measurements of lung osmosis and filtration. The effects of aquaporin gene deletion, mercurials, and temperature on lung water transport provide experimental evidence that unstirred layers are of little concern. Vascular compliance is a potential complicating factor, particularly in filtration measurements where perfusate inflow and/or outflow pressure are changed. In mouse lung, it appears easier to resolve vascular versus fluid accumulation phases of weight change than in reported dog lung experiments. Vascular compliance is probably of little concern in measurements of osmotic water permeability as experimentally verified by the monophasic changes in lung weight in response to changes in perfusate osmolality. Last, based on preliminary experiments, we note that gravimetry appears to be useful to measure osmosis and filtration in other perfused mouse organs such as liver and brain.

Although the present study examined the role of AQP4 in lung water transport, it did not provide direct measurements of airway water permeability, nor did it address the broader issue of the role of aquaporins in lung physiology. Methodologies are needed to measure apical and basolateral water permeabilities in distal airways from mice. Studies to address aquaporin physiology in lung are in progress, including measurements of active alveolar fluid clearance in the adult lung, neonatal lung fluid clearance, and lung edema in various injury models such as acid aspiration, congestive heart failure and hyperoxia. These studies are being done using the AQP1 and AQP4 knockout mice, as well as knockout mice with deletions of AQP3 expressed in large airways, and AQP5 expressed in alveolar epithelium. It is notable here that the AQP1/AQP4 double knockout mice, although less robust than wild-type or AQP1 null mice, are able to survive and generally grow well. The residual low water permeability in lung after AQP1 and AQP4 deletion thus appears to be adequate for mice to survive and thrive. Further experiments as described above and using mice containing multiple aquaporin gene deletions will be required to define the role of aquaporins in lung physiology under normal and pathological conditions.

We thank Ms. Liman Qian for transgenic mouse breeding and genotype analysis.

This study was supported by National Institutes of Health grants HL59198, HL51854, DK35124, HL60288, and DK43840, and grant R613 from the National Cystic Fibrosis Foundation.

Submitted: 30 July 1999
Revised: 28 October 1999
Accepted: 1 November 1999
Released online: 13 December 1999

Note Added in Proof. AQP4 knockout mice also manifest reduced brain edema in response to water intoxication and ischemic stroke (Manley, G.T., M. Fujimora, T. Ma, N. Noshita, F. Feliz, A.W. Bollen, P. Chan, and A.S. Verkman. 2000. Aquaporin-4 deletion in mice reduces brain edema following acute water intoxication and ischemic stroke. *Nat. Med.* In press).

REFERENCES

Agostoni, E., and J. Piiper. 1962. Capillary pressure and distribution of vascular resistance in isolated lung. *Am. J. Physiol.* 202:1033–1036.

Annernarie, G., and E.R. Weibel. 1971. Morphometric estimation of pulmonary diffusion capacity. *Respir. Physiol.* 11:354–366.

Bai, C., N. Fukuda, Y. Song, T. Ma, M.A. Matthay, and A.S. Verkman. 1999. Lung fluid transport in aquaporin-1 and aquaporin-4 knockout mice. *J. Clin. Invest.* 103:555–561.

Carter, E.P., M.A. Matthay, J. Farinas, and A.S. Verkman. 1996. Transalveolar osmotic and diffusional water permeability in intact mouse lung measured by a novel surface fluorescence method. *J. Gen. Physiol.* 108:133–142.

Carter, E.P., B.P. Ölveczky, M.A. Matthay, and A.S. Verkman. 1998. High microvascular endothelial water permeability in mouse lung measured by a pleural surface fluorescence method. *Biophys. J.* 74:2121–2128.

Carter, E.P., F. Umenishi, M.A. Matthay, and A.S. Verkman. 1997. Developmental changes in alveolar water permeability in perinatal rabbit lung. *J. Clin. Invest.* 100:1071–1078.

Chou, C.L., M.A. Knepper, A.N. van Hoek, D. Brown, B. Yang, T. Ma, and A.S. Verkman. 1999. Reduced water permeability and altered ultrastructure in thin descending limb of Henle in aquaporin-1 null mice. *J. Clin. Invest.* 103:491–496.

Chou, C.L., T. Ma, B. Yang, M.A. Knepper, and A.S. Verkman. 1998. Four-fold reduction in water permeability in inner medullary collecting duct of aquaporin-4 knockout mice. *Am. J. Physiol.* 274: C549–C554.

Dobbs, L., R. Gonzalez, M.A. Matthay, E.P. Carter, L. Allen, and A.S.

Verkman. 1998. Highly water-permeable type I alveolar epithelial cells confer high water permeability between the airspace and vasculature in rat lung. *Proc. Natl. Acad. Sci. USA.* 95:2991–2996.

Drake, R.E., J.H. Smith, and J.C. Gable. 1980. Estimation of the filtration coefficient in intact dog lungs. *Am. J. Physiol.* 238:H430–H438.

Effros, R.M., C. Darin, E.R. Jacobs, R.A. Rogers, G. Krenz, and E.E. Schneeberger. 1997. Water transport and distribution of aquaporin-1 in the pulmonary airspaces. *J. Appl. Physiol.* 83:1002–1016.

Ehrhard, J.C., W.M. Granger, and W.F. Hofman. 1984. Filtration coefficient obtained by stepwise pressure elevation in isolated dog lung. *J. Appl. Physiol.* 56:862–867.

Folkesson, H., M. Matthay, A. Frigeri, and A.S. Verkman. 1996. High transepithelial water permeability in microperfused distal airways: evidence for channel-mediated water transport. *J. Clin. Invest.* 97:664–671.

Folkesson, H.G., M.A. Matthay, H. Hasegawa, F. Kheradmand, and A.S. Verkman. 1994. Transcellular water transport in lung alveolar epithelium through mercury-sensitive water channels. *Proc. Natl. Acad. Sci. USA.* 91:4970–4974.

Frigeri, A., M. Gropper, C.W. Turck, and A.S. Verkman. 1995. Immunolocalization of the mercurial-insensitive water channel and glycerol intrinsic protein in epithelial cell plasma membranes. *Proc. Natl. Acad. Sci. USA.* 92:4328–4331.

Funaki, H., T. Yamamoto, Y. Koyama, D. Kondo, E. Yaoita, K. Kawasaki, H. Kobayashi, S. Sawaguchi, H. Abe, and I. Kihara. 1998. Localization and expression of AQP5 in cornea, serous salivary glands and pulmonary epithelial cells. *Am. J. Physiol.* 275:C1151–C1157.

Gaar, K.A., A.E. Taylor, L.J. Owens, and A.C. Guyton. 1967. Pulmonary capillary pressure and filtration coefficient in the isolated perfused lung. *Am. J. Physiol.* 213:910–914.

Harris, N.R., R.E. Parker, N.A. Pou, and R.J. Roselli. 1992. Canine pulmonary filtration coefficient calculated from optical, radioisotope and weight measurements. *J. Appl. Physiol.* 73:2648–2661.

Horsfield, K. 1981. The structure of the tracheobronchial tree. *In* Scientific Foundations of Respiratory Medicine. J.G. Scadding and G. Cumming, editors. W.B. Saunders Co., Philadelphia, PA. 54–70.

King, L.S., S. Nielsen, and P. Agre. 1997. Aquaporins in complex tissues. I. Developmental patterns in respiratory and glandular tissues of rat. *Am. J. Physiol.* 273:C1541–C1548.

King, L.S., S. Nielsen, and P. Agre. 1996. Aquaporin-1 water channel protein in lung-ontogeny, steroid-induced expression, and distribution in rat. *J. Clin. Invest.* 97:2183–2191.

Ma, T., N. Fukuda, Y. Song, M.A. Matthay, and A.S. Verkman. 2000. Lung fluid transport in aquaporin-5 knockout mice. *J. Clin. Invest.* In press.

Ma, T., Y. Song, A. Gillespie, E.J. Carlson, C.J. Epstein, and A.S. Verkman. 1999. Defective secretion of saliva in transgenic mice lacking aquaporin-5 water channels. *J. Biol. Chem.* 274:20071–20074.

Ma, T., B. Yang, A. Gillespie, E.J. Carlson, C.J. Epstein, and A.S. Verkman. 1997. Generation and phenotype of a transgenic knock-out mouse lacking the mercurial-insensitive water channel aquaporin-4. *J. Clin. Invest.* 100:957–962.

Ma, T., B. Yang, A. Gillespie, E.J. Carlson, C.J. Epstein, and A.S. Verkman. 1998. Severely impaired urinary concentrating ability in transgenic mice lacking aquaporin-1 water channels. *J. Biol. Chem.* 273:4296–4299.

Matalon, S., R.J. Bridges, and D.J. Benos. 1991. Amiloride-inhibitable Na^+ conductive pathways in alveolar type II pneumocytes. *Am. J. Physiol.* 260:L90–L96.

Matthay, M.A., H. Folkesson, and A.S. Verkman. 1996. Salt and water transport across alveolar and distal airway epithelia in the adult lung. *Am. J. Physiol.* 270:L487–L503.

Maya, S. 1991. Lung endothelium: structure-function correlates. *In* The Lung, Scientific Foundations. R.G. Crystal and J.B. West, editors. Raven Press, New York, NY. 301–312.

Murry, J.F. 1986. The Normal Lung. W.B. Sanders Co. Philadelphia, PA. 23–59.

Nielsen, S., B.L. Smith, E.I. Christensen, and P. Agre. 1993. Distribution of the aquaporin CHIP in secretory and resorptive epithelia and capillary endothelia. *Proc. Natl. Acad. Sci. USA.* 90:7275–7279.

Pallone, T.L., A. Edwards, T. Ma, E. Sildorff, and A.S. Verkman. 2000. Requirement of aquaporin-1 for NaCl driven water transport across descending vasa recta. *J. Clin. Invest.* In press.

Pappenheimer, J.R., and A. Soto-Rivera. 1948. Effective osmotic pressure of the plasma proteins and other quantities associated with the capillary circulation in the hindlimbs of cats and dogs. *Am. J. Physiol.* 152:471–490.

Parker, J.C., R. Prasad, R.A. Allison, W.V. Wojchiechowski, and S.L. Martin. 1993. Capillary filtration coefficients using laser densitometry and gravimetry in isolated dog lungs. *J. Appl. Physiol.* 74: 1981–1987.

Schnermann, J., J. Chou, T. Ma, M.A. Knepper, and A.S. Verkman. 1998. Defective proximal tubule reabsorption in transgenic aquaporin-1 null mice. *Proc. Natl. Acad. Sci. USA.* 95:9660–9664.

Simionescu, M. 1991. Lung endothelium: structure–function correlates. *In* The Lung: Scientific Foundation. Vol. 1. R.G. Crystal and J.B. West, editors. Raven Press, New York, NY. 301–312.

Umenishi, F., E.P. Carter, B. Yang, B. Oliver, M.A. Matthay, and A.S. Verkman. 1996. Sharp increase in rat lung water channel expression in the perinatal period. *Am. J. Respir. Cell Mol. Biol.* 15:673–679.

Verkman, A.S. 2000. Water permeability measurement in living cells and complex tissues. *J. Member. Biol.* In press.

Weibel, E.R. 1989. Lung morphometry and models in respiratory physiology. *In* Respiratory Physiology. H.K. Chang and M. Pavia, editors. Marcel Dekker, New York, NY. 1–56.

Yasui, M., E. Serlachius, M. Lofgren, R. Belusa, S. Nielsen, and A. Aperia. 1997. Perinatal changes in expression of aquaporin-4 and other water and ion transporters in rat lung. *J. Physiol.* 505:3–11.